JARO 5: 99–110 (2004)
DOI: 10.1007/s10162-003-4022-1

JARO
Journal of the Association for Research in Otolaryngology

# Low Endolymph Calcium Concentrations in *deafwaddler*$^{2J}$ Mice Suggest that PMCA2 Contributes to Endolymph Calcium Maintenance

J. David Wood,[1,2] Sara J. Muchinsky,[1,3] Adelaida G. Filoteo,[4] John T. Penniston,[4] and Bruce L Tempel[1,2,3]

[1]*The Virginia Merrill Bloedel Hearing Research Center, University of Washington School of Medicine, Seattle, WA 98195-7923, USA*
[2]*Department of Otolaryngology-Head and Neck Surgery, University of Washington School of Medicine, Seattle, WA 98195, USA*
[3]*Department of Pharmacology, University of Washington School of Medicine, Seattle, WA 98195, USA*
[4]*Department of Biochemistry and Molecular Biology, Mayo Foundation, Rochester, MN 55905, USA*

Received: 13 June 2003; Accepted: 24 October 2003; Online publication: 4 May 2004

## ABSTRACT

In vertebrates, transduction of sound into an electrochemical signal is carried out by hair cells that rely on calcium to perform specialized functions. The apical surfaces of hair cells are surrounded by endolymphatic fluid containing calcium at concentrations that must be maintained by active transport. The mechanism of this transport is unknown, but an ATP-dependent pump is believed to participate. Mutation of the *Atp2b2* gene that encodes plasma membrane calcium ATPase type 2 (PMCA2) produces the deaf, ataxic mouse: deafwaddler$^{2J}$ (*dfw*$^{2J}$). We hypothesized that PMCA2 might transport calcium into the endolymph and that *dfw*$^{2J}$ mice would have low endolymph calcium concentrations, possibly contributing to their deafness and ataxia. First, using immunocytochemistry, we demonstrated that PMCA2 is present in control mice inner and outer hair cell stereocilia where it could pump calcium into the endolymph and that PMCA2 is absent in *dfw*$^{2J}$ stereocilia. Second, using an aspirating microelectrode and calcium-sensitive fluorescent dye, we found that *dfw*$^{2J}$ mice endolymph calcium concentrations are significantly lower than those of control mice. These findings suggest that PMCA2, located in hair cell stereocilia, contributes significantly to endolymph calcium maintenance.

**Keywords:** PMCA2, endolymph, calcium, deafwaddler, *Atp2b2*

## INTRODUCTION

Auditory hair cells convert sound into an electrochemical signal by a process called transduction. At the hair cell's apical surface, actin-filled, filamentous stereocilia are arranged in parallel rows of increasing length that extend into the scala media (reviewed in Hudspeth 1997). Endolymphatic fluid surrounds the stereocilia and apical surface of hair cells. Sound causes deflection of stereocilia that, when directed towards the tallest stereocilium, opens cation-selective transduction channels, allowing endolymph potassium ($K^+$) and calcium ($Ca^{2+}$) to flow into and depolarize the hair cells (Lumpkin et al. 1997; Ricci and Fettiplace 1998).

*In vitro* studies indicate that $Ca^{2+}$ regulates several hair cell functions. Bullfrog saccular maculae hair cell transduction channels have been shown to be selective for $Ca^{2+}$ over monovalent cations (Lumpkin et al. 1997). In ionic environments approximating endolymph, $Ca^{2+}$ carries as much as 20% of turtle auditory hair cell transduction currents (Ricci and Fettiplace

*Correspondence to:* Bruce L Tempel • V.M. Bloedel Hearing Research Center • Box 357923 • University of Washington • Seattle, WA 98195-7923 • Telephone: (206) 616-4693; Fax: (206) 616-1828; email: bltempel@u.washington.edu

1998). Generation of stable transduction currents in chick vestibular hair cells requires minimum extracellular $Ca^{2+}$ concentrations of 20 $\mu$M, and transduction currents are not elicitable in 10 $\mu$M extracellular calcium (Ohmori 1985). Bullfrog macular epithelium microphonic currents, produced by deflecting hair bundles, also require greater than 10 $\mu$M extracellular $Ca^{2+}$ (Corey and Hudspeth 1979). Bundle stiffening is diminished (Ricci et al. 2000) and adaptation is slowed (Assad et al. 1989; Ricci and Fettiplace 1998) when extracellular calcium concentrations are reduced.

*In vivo* observations suggest that maintenance of endolymph $Ca^{2+}$ is necessary for normal hearing. Application of EDTA, a $Ca^{2+}$ chelating agent, to the scala media suppresses cochlear microphonics (Tanaka et al. 1979; Marcus et al. 1982). Rats with hypocalcemia secondary to vitamin D deprivation exhibit depressed cochlear microphonic amplitudes and elevated thresholds (Ikeda et al. 1987a). In humans, vitamin D deficiency (Brookes 1985; Ikeda et al. 1989), renal failure (Bergstrom et al. 1973; Johnson and Mathog 1976), and hypoparathyroidism (Ikeda et al. 1987b)—conditions that cause low serum and presumed low endolymph $Ca^{2+}$ concentrations—are associated with sensorineural hearing loss.

In wild-type rats, endolymph $Ca^{2+}$ concentrations have been reported as 20–30 $\mu$M (Bosher and Warren 1978; Salt 1986; Ferrary et al. 1988). The concentration of $Ca^{2+}$ in mammalian endolymph is low relative to perilymph and other extracellular fluids, but given the strongly positive endocochlear potential (EP), which drives cations out of the endolymph, $Ca^{2+}$ is present in concentrations much higher than predicted by passive distribution. In the rat, based on Bosher's measured perilymph calcium concentration of 640 $\mu$M and the endocochlear potential, the Nernst equation predicts that the endolymph $Ca^{2+}$ concentration should be 0.7 $\mu$M, but measured concentrations are 25–40 times higher. In the chinchilla, $Ca^{2+}$ has been shown to have a 20.2 mV electrochemical potential gradient from the perilymph to the endolymph (Ikeda et al. 1988). These observations indicate that $Ca^{2+}$ is actively transported into the endolymph, but neither the mechanism nor the site of transport is known.

Two families of proteins are known to extrude $Ca^{2+}$ from cells: sodium/calcium exchangers and calcium ATPases (Carafoli 1987; Miller 1991). Sodium/$Ca^{2+}$ exchangers rely on elevated extracellular sodium concentrations to transport $Ca^{2+}$ out of cells, but endolymph sodium concentrations are low, approximating those of intracellular fluid. Furthermore, amiloride, a sodium/$Ca^{2+}$ exchanger inhibitor, does not lower endolymph calcium concentrations (Ikeda et al. 1988). Application of vanadate, an ATPase antagonist, to the round window has been shown to decrease endolymph $Ca^{2+}$ concentrations and eliminate the $Ca^{2+}$ electrochemical potential gradient in chinchillas, suggesting that a calcium ATPase maintains endolymph $Ca^{2+}$ (Ikeda et al. 1987a, 1988). Vanadate has also been shown to inhibit extrusion of $Ca^{2+}$ from the apical surface of isolated bullfrog saccular hair bundles that normally lie in endolymph (Yamoah et al. 1998).

Molecules capable of transporting $Ca^{2+}$ into the endolymph must be present in the apical surface of the endolumenal cell layer whose ion-impermeable tight junctions isolate the endolymph from the surrounding perilymph (Jahnke 1975). The endolumenal layer is comprised of interdental, hair, Hensen, Claudius, external sulcus, stria vascularis, and Reissner's membrane cells.

PMCA is a plasma membrane protein that, in mammals, exists in four known types (PMCA1–4) encoded by four different genes each of which undergoes alternative exon splicing in regions A and C (Keeton et al. 1993). All four PMCA types have been demonstrated in the mammalian cochlea (Crouch and Schulte 1996). In the endolumenal layer, immunocytochemistry (ICC) has identified PMCA2a in inner and outer rat hair cell bundles (Dumont et al. 2001). In addition, *in situ* hybridization has demonstrated PMCA1 mRNA in rat stria vascularis (Furuta et al. 1998), and non-type-specific PMCA ICC has suggested that PMCA protein is present in gerbil and guinea pig stria vascularis (Crouch and Schulte 1995; Agrup et al. 1999).

The deafwaddler$^{2J}$ ($dfw^{2J}$) mutant mouse exhibits profound deafness (Noben–Trauth et al. 1997), vestibular dysfunction, and a wobbling gait. The $dfw^{2J}$ phenotype results from a two-base-pair deletion in the *Atp2b2* gene that encodes PMCA2. This mutation produces a frame shift and premature protein truncation after amino acid 471 (Street et al. 1998). Although anatomic abnormalities, including decreased numbers of stereocilia and compressed tunnels of Corti, have been observed in $dfw^{2J}$ (Street et al. 1998), the pathophysiology underlying the mutant's phenotype is not fully understood.

Given the importance of $Ca^{2+}$ for hair cell function, the evidence that a calcium ATPase maintains endolymphatic calcium, and the knowledge that mutation of PMCA2 produces a profoundly deaf mouse, we hypothesized that PMCA2 maintains endolymph $Ca^{2+}$ and that $dfw^{2J}$ mice would have low endolymph calcium concentrations. To investigate this hypothesis, we used immunocytochemistry to determine which PMCA isoforms are present in endolumenal cells where they might pump calcium into the endolymph, and we measured the endolymph $Ca^{2+}$ concentrations of $dfw^{2J}$ and control mice.

## MATERIALS AND METHODS

### Animals

Deafwaddler$^{2J}$ mice in the BALB/c background were obtained from Jackson Labs and transferred into the CBA background via serial backcrosses to CBA/CaJ mice for five generations to produce the CBA/CaJ-*Atp2b2*$^{dfw2J}$ congenic strain that we refer to here as $dfw^{2J}$. CBA/CaJ (CB) mice were used as controls. For the anatomic and immunocytochemistry studies, all animals were postnatal day 30. For the calcium and EP measurement experiments, all animals were between 4 and 6 weeks old. All procedures were approved by the University of Washington Institutional Animal Care and Use Committee.

### PMCA type localization

PMCA-type-specific antibodies NR1, NR2, and NR3 are polyclonal antibodies specific for PMCA1, PMCA2, and PMCA3, respectively (Filoteo et al. 1997). All NR antibodies were used with a goat-anti-rabbit biotinylated secondary antibody (Vector Laboratories, Burlingame, CA). JA9 is a monoclonal antibody specific for PMCA4 (Caride et al. 1996). 5F10 (Affinity Bioreagents, Inc., Golden, CO) is a monoclonal antibody that recognizes all known PMCA types. JA9 and 5F10 were used with a goat-anti-mouse biotinylated secondary antibody (Sigma, St. Louis, MO). PMCA1–PMCA4 antibodies were diluted 1:250, and 5F10 was diluted 1:500 in nonspecific blocking buffer (3% BSA, 3% goat serum, and 0.2% Triton X-100). All antibody and blocking buffer incubations were performed at 4°C.

For each antibody, one $dfw^{2J}$ and one CB cochlea were reacted in whole mount, embedded in plastic, and sectioned to provide high anatomic resolution. Two cochleae from each genotype were embedded in paraffin, sliced, and mounted prior to antibody exposure to allow use of multiple antibodies in each cochlea. Mice were killed by carbon dioxide exposure, and the cochleae were removed and fixed with 4% paraformaldehyde. The specimens were then decalcified in 0.5 M EDTA at 4°C for 4 days. All sections were analyzed by light microscopy.

**Plastic sections.** After decalcification, a midmodiolar cut was made, and the cochleae were immersed in 0.25% $H_2O_2$ for 30 min. Cochleae were washed in phosphate-buffered saline (PBS), incubated in nonspecific blocking buffer overnight, and covered with primary antibodies for 96 h. Negative controls were prepared with no primary antibody. Following PBS rinses, cochleae were incubated in secondary antibody for 24–36 h. After rinsing with PBS, specimens were incubated in Vectastain Elite ABC solution (Vector Laboratories) for 24–36 h, washed in PBS, and developed with diaminobenzidine tetrahydrochloride (DAB) for 45 min. Then, the cochleae were embedded in Spurr's plastic (Ted Pella, Inc., Reddington, CA), sectioned to 3 $\mu$m thickness, and analyzed.

**Paraffin sections.** After decalcification, cochleae were dehydrated through a graded series of alcohols, embedded in Paraplast Plus (3 × 2 h at 58°C; Curtis Matheson, Houston, TX), sectioned at 7 $\mu$m, and collected onto glass slides. Sections were deparaffinized, rehydrated through a graded series of xylenes and alcohols, and incubated in 0.25% $H_2O_2$ for 30 min at room temperature. After washes in PBS, the sections were incubated in nonspecific blocking buffer for 30 min. Next, they were incubated with primary antibodies for 48 h rinsed with PBS, and incubated with secondary antibodies for 1 h. After PBS rinses, sections were incubated in ABC solution at room temperature for 1 h, rinsed with PBS, developed with DAB, and analyzed.

**Anatomy analysis.** Plastic sections from negative controls were examined to assess $dfw^{2J}$ and CB cochlear anatomy. Each section was evaluated for intactness of the cochlear duct, tunnel of Corti, stria vascularis, inner and outer hair and support cells, and stereocilia.

### Endolymph $Ca^{2+}$ and endocochlear potential measurements

A microaspiration/microelectrode (aspirode) device was designed to collect a sample of endolymph while simultaneously monitoring the endocochlear potential. The presence of an EP was used to verify placement of the aspirode in the scala media, and stability of the EP during aspiration was monitored to verify the integrity of the cochlear duct. Disruption of the cochlear duct would allow free exchange of ions between the endolymph and perilymph, rapidly depleting the EP and contaminating the sample with $Ca^{2+}$-rich perilymph.

Double-barrel, 1.5-mm-inner-diameter, glass capillaries with internal filaments (World Precision Instruments, Sarasota, Fl) were pulled with a David Kopf Instruments (Tujunga, CA) model 700c vertical puller at a solenoid setting of 20 and a current of 19 A. Tips were subsequently broken to an individual barrel inner diameter of 2.5 $\mu$m and a total width of 10 $\mu$m. One of the barrels was connected to a tuberculin syringe using polyethylene tubing (outer diameter: 0.61 mm, inner diameter: 0.28 mm) (Becton Dickson, Franklin Lakes, NJ) attached with epoxy resin glue. The other barrel was filled with 18.2 M$\Omega$, purified water. Using a Hamilton gas-tight syringe, 0.4 $\mu$L of purified water was then dispensed onto a glass slide. This calibration sample was drawn into the

aspirating barrel by applying negative pressure with the syringe, the height of the meniscus was marked, and the sample expelled. Aspirodes were allowed to dry overnight, and the electrode barrel was filled with 0.5 M KCl into which a 0.013 in. diameter silver chloride wire was inserted and attached to a voltmeter. A silver chloride ground wire was placed in the animal's neck musculature and connected to the voltmeter.

A custom $Ca^{2+}$ quantification well was fashioned from polystyrene and glass and filled with low-fluorescence immersion oil (Cargille Laboratories Inc., Cedar Grove, NJ). Fluorescent dye was aspirated to the calibration mark in the aspirode to be used and was injected into the bottom of the well forming a bubble. The ratiometric, $Ca^{2+}$-sensitive dye Fura FF (Molecular Probes, Eugene, OR) and fluorescence microscopy were used to measure endolymph sample $Ca^{2+}$ concentrations, based on a $K_d$ derived from a 1–500 $\mu$M calcium standard calibration curve (Molecular Probes).

### Surgery

Mice were rapidly anesthetized with ketamine/xylazine, and endolymph was aspirated from both cochleae. First, the skull was fixed to a stabilization bar, and the pinna and posterior auditory canal wall were resected to expose the basal turn of the cochlea. A small hole was made in the otic capsule, exposing the spiral ligament, and using a micromanipulator, the aspirode tip was advanced to just touch the spiral ligament. The voltmeter was zeroed, the aspirode was advanced through the spiral ligament until a stable EP was measured, and fluid was aspirated to the calibration mark. The EP was monitored throughout the aspiration; if it changed more than 10 mV, the sample was discarded. Accepted samples were transferred to the bottom of the Fura FF preloaded well.

The well was placed on the stage of a fluorescence microscope, and the edge of the sample bubble was brought into sharp focus. The objective was centered in the bubble, and a 75 W xenon short arc lamp excited the sample at 340 and 380 nm. The resulting 510 nm fluorescence was measured and the $R$ value determined with an intensified CCD camera (Hamamatsu Photonics, Hamamatsu, Japan) and Metafluor (SDR Clinical Technology, Sydney, Australia). The entire process of focusing, recentering, and determining the $R$ value was repeated three times for each sample, and the $R$ value average was used to calculate the $Ca^{2+}$ concentration according to the formula: $[Ca^{2+}] = K_d Q(R-R_{min})/(R_{max}-R)]$. The concentration was then corrected for dilution in Fura FF.

Aspirodes were originally calibrated with 1 $\mu$L of water. Aspiration to this calibration mark resulted in a rapid decline of the EP presumably due to cochlear duct rupture. A smaller calibration volume of 0.4 $\mu$L was adopted, resulting in stable EPs. To more accurately determine the volume of endolymph withdrawn by aspirodes calibrated with this volume, aspirodes used in the experiments were filled to their calibration mark with water that was then ejected into a preweighed microfuge cap (Eppendorf, Hamburg, Germany) filled with mineral oil. This process was repeated ten times and the cap was reweighed. The original cap and mineral oil weight was subtracted from the result and the difference was used to calculate the sample's total volume based on a water density of 0.997542 g/ml at 23°C. The result was divided by 10 to determine the individual sample volume. Volumes calculated from five different aspirodes used in these studies ranged from 0.21 to 0.25 $\mu$L, slightly larger than the cochlear duct volume measured by magnetic resonance imaging of a mouse (Thome et al. 1999).

## RESULTS

### Anatomy

Microscopy revealed anatomic abnormalities of varying severity in each *dfw*$^{2J}$ cochlea. All cochleae contained areas that appeared normal with intact inner and outer hair cells, tunnels of Corti, support cells, and stereocilia (Fig. 1A, B). Variable portions of each *dfw*$^{2J}$ cochlea, however, exhibited collapsed tunnels of Corti, poorly defined cell types, and unidentifiable stereocilia (Fig. 1C, D). Reissner's membrane was occasionally disrupted in both *dfw*$^{2J}$ and CB cochlea sections but was always intact in some sections from each cochlea.

### Immunohistochemistry

Wild-type mice demonstrated prominent PMCA1 labeling of inner hair cell basolateral membranes (Table 1; Fig. 2, NR1 CB; Fig. 4, CB). Though cellular resolution was somewhat limited by the intensity of staining, PMCA1 labeling appeared to be present around the entire plasma membrane of the stria vascularis marginal cells that surround the scala media (Table 1; Fig. 3A, NR1 CB; Fig. 4, CB). Interdental cells, lining the furrows between spiral limbus Hushke's teeth, were also intensely labeled for PMCA1 (Table 1; Fig. 3B, NR1 CB; Fig. 4, CB). *dfw*$^{2J}$ mice demonstrated similar stria and interdental cell PMCA1 labeling (Table 1; Fig. 3A, NR1 *dfw*$^{2J}$; Fig. 3B, NR1 *dfw*$^{2J}$; Fig. 4, *dfw*$^{2J}$), but inner hair cell labeling in the mutants was apical rather than basolateral (Table 1; Fig. 2, NR1 *dfw*$^{2J}$; Fig. 4, *dfw*$^{2J}$). *dfw*$^{2J}$ mice also exhibited apical outer hair cell staining not observed

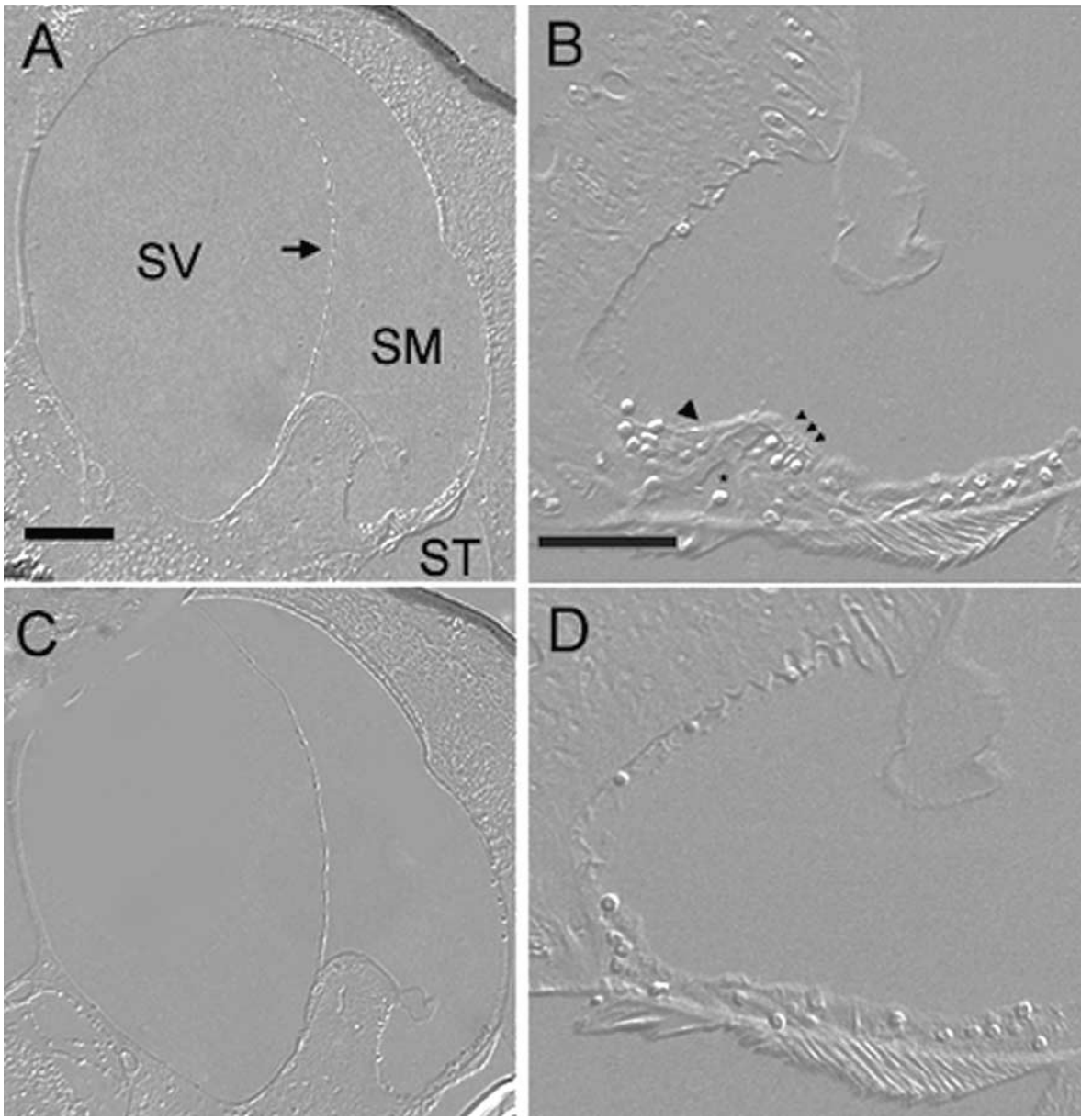


**FIG. 1.** *dfw*$^{2J}$ anatomy. Examples of the most normal and abnormal cochlear anatomy in a single *dfw*$^{2J}$ mouse. **A, B** Sections with relatively intact anatomy, viewed at 10× and 40×. The tunnel of Corti, Reissner's membrane, and inner and outer hair cells appear normal. **C, D** Sections with distorted anatomy, viewed at 10× and 40×. The tunnel of Corti and hair cells are not identifiable. All sections are embedded in plastic, 3 $\mu$m thick, and viewed with Nomarski optics. SM, scala media; SV, scala vestibuli; ST, scala tympani; arrow, Reissner's membrane; large arrow head, inner hair cell; small arrow heads, outer hair cells; *, tunnel of Corti. Scale bar = 50 $\mu$m for **A** and **C** and 20 $\mu$m for **B** and **D**.

in wild-type mice (Table 1; Fig. 2, NR1 *dfw*$^{2J}$; Fig. 4, *dfw*$^{2J}$). Low-intensity, diffuse PMCA1 labeling was present occasionally in *dfw*$^{2J}$ and CB Hensen and external sulcus cells (Table 1; Fig. 4, CB and *dfw*$^{2J}$).

In CB mice, PMCA2 labeling was present at high levels in outer hair cell stereocilia and apical membranes and at moderate levels in inner hair cell stereocilia (Table 1; Fig. 2, NR2 CB; Fig. 4, CB). No PMCA2 immunostaining was observed in *dfw*$^{2J}$ mice (Table 1; Fig. 2, NR2 *dfw*$^{2J}$; Fig. 3A, NR2 *dfw*$^{2J}$; Fig. 4, *dfw*$^{2J}$). Given the NR2 antibody's recognition of an epitope upstream of the mutant's protein truncation, this result confirms that *dfw*$^{2J}$ is, effectively, a null mutation without expression of the truncated protein (Street et al. 1998).

Immunostaining for PMCA3 was not observed in CB or *dfw*$^{2J}$ cochleae (Table 1). Moderate PMCA4 labeling was present in the inner and outer hair cell stereocilia of *dfw*$^{2J}$ mice but was not observed in wild-type animals (Table 1; Fig. 2, JA9 CB and JA9 *dfw*$^{2J}$; Fig. 4, CB and *dfw*$^{2J}$). Consistent with its recognition of all four PMCA types, 5F10 labeled all structures

**TABLE 1**

PMCA ICC summary[a]

| | *NR1* | *NR2* | *NR3* | *JA9* | *5F10* |
|---|---|---|---|---|---|
| IHC | | | | | |
| CB | +++(blm) | 0 | 0 | 0 | +++(blm) |
| *dfw*$^{2J}$ | +++(am) | 0 | 0 | 0 | +++(am) |
| IHC SC | | | | | |
| CB | 0 | ++ | 0 | 0 | ++ |
| *dfw*$^{2J}$ | 0 | 0 | 0 | ++ | ++ |
| OHC | | | | | |
| CB | 0 | +++(am) | 0 | 0 | +++(am) |
| *dfw*$^{2J}$ | +++(am) | 0 | 0 | 0 | +++(am) |
| OHC SC | | | | | |
| CB | 0 | +++ | 0 | 0 | *+++* |
| *dfw*$^{2J}$ | 0 | 0 | 0 | ++ | ++ |
| HC | | | | | |
| CB | + | 0 | 0 | 0 | + |
| *dfw*$^{2J}$ | + | 0 | 0 | 0 | + |
| ESC | | | | | |
| CB | + | 0 | 0 | 0 | + |
| *dfw*$^{2J}$ | + | 0 | 0 | 0 | + |
| SV | | | | | |
| CB | +++ | 0 | 0 | 0 | +++ |
| *dfw*$^{2J}$ | +++ | 0 | 0 | 0 | +++ |
| RM | | | | | |
| CB | 0 | 0 | 0 | 0 | 0 |
| *dfw*$^{2J}$ | 0 | 0 | 0 | 0 | 0 |
| IC | | | | | |
| CB | +++ | 0 | 0 | 0 | +++ |
| *dfw*$^{2J}$ | +++ | 0 | 0 | 0 | +++ |

[a]Summary of labeling produced by PMCA antibodies: NR1 (PMCA1), NR2 (PMCA2), NR3 (PMCA3), JA9 (PMCA4), 5F10 (all PMCA types). 0, no labeling; +, low labeling; ++, moderate labeling; +++, intense labeling; am, apical membrane; blm, basolateral membrane; HC, Hensen cells; IHC, inner hair cell; IHC SC, inner hair cell stereocilia; OHC, outer hair cell; OHC SC, outer hair cell stereocilia; ESC, external sulcus cells; SV, stria vascularis; RM, Reissner's membrane; IC, interdental cells.

identified by NR1–3 and JA9 in both CB and *dfw*$^{2J}$ mice, with no labeling of other structures (Table 1). There was infrequent low-intensity labeling of Reissner's membrane by all five antibodies but no consistent labeling with any single antibody. We interpret our inconsistent labeling of Reissner's membrane as an artifact. However, others have reported prominent 5F10 labeling of Reissner's membrane in the developing gerbil and low-level labeling in the adult (Crouch and Schulte 1995; Agrup et al. 1999). In addition, *in situ* hybridization experiments have suggested moderate levels of PMCA2 mRNA in the adult rat Reissner's membrane (Furuta et al. 1998). These differences may be due to interspecies variation, differing techniques, or differences in threshold criteria.

## Endolymph calcium concentrations

The mean endolymph $Ca^{2+}$ concentration in control animals was 22.9 ± 3.5 $\mu$M ($n$ = 8; all means are presented as mean ± standard error; Fig. 5A), consistent with previous measurements in the rat of 23 $\mu$M (Bosher and Warren 1978). With the possible exception of one $Ca^{2+}$ measurement of 42.3 $\mu$M, there was no evidence of contamination by $Ca^{2+}$-rich perilymph, indicating that our technique is effective in selectively measuring endolymph calcium concentration. The mean endolymph calcium concentration of *dfw*$^{2J}$ mice was 6.6 ± 0.6 $\mu$M ($n$ = 8, Fig. 5A). The difference between *dfw*$^{2J}$ and CB $Ca^{2+}$ concentrations was statistically significant with a $p$ value of 0.001 determined by the two-tailed Student's $t$ test. Of all the wild-type animals, the largest difference between the three measurements made of each sample was 11 $\mu$M. Most measurements were tighter and the next largest variabilities were 6.2 and 4.6 $\mu$M. Among *dfw*$^{2J}$ animals, the largest difference in measurements of a single sample was 2.6 $\mu$M.

## Endocochlear potentials

Including initial experiments to develop EP and $Ca^{2+}$ measurement techniques, stable EPs were recorded

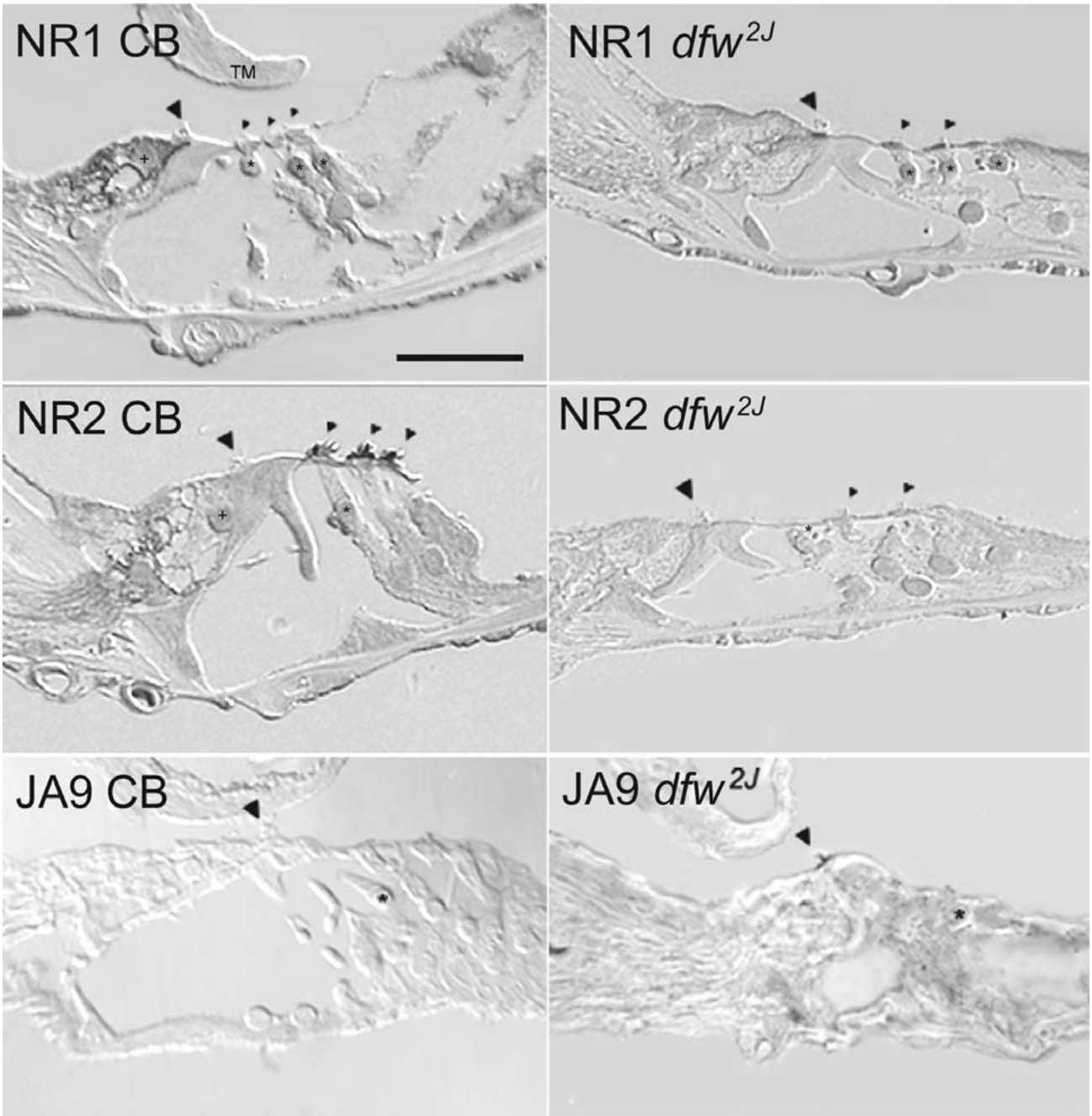


**FIG. 2.** PMCA1, PMCA2, and PMCA4 staining in the organ of Corti. **NR1 CB** NR1 immunocytochemistry (ICC) for PMCA1 in CB organ of Corti. There is intense NR1 labeling of the inner hair cell basolateral membrane. There is no NR1 labeling of outer hair cells. **NR1 *dfw*$^{2J}$** NR1 ICC for PMCA1 in *dfw*$^{2J}$ organ of Corti. NR1 labeling is concentrated at inner and outer hair cell apical surfaces with minimal basolateral labeling. **NR2 CB** NR2 labeling for PMCA2 in CB organ of Corti. There is prominent NR2 labeling of outer hair cell stereocilia (moderate labeling of inner hair cell stereocilia is more prominent in other sections). **NR2 *dfw*$^{2J}$** NR2 labeling for PMCA2 in *dfw*$^{2J}$ organ of Corti. There is no NR2 labeling of the stereocilia. **JA9 CB** JA9 labeling for PMCA4 in CB organ of Corti. There is no JA9 labeling of the CB organ of Corti. **JA9 *dfw*$^{2J}$**. JA9 labeling for PMCA4 in *dfw*$^{2J}$ organ of Corti. There is moderate labeling of inner hair cell stereocilia (labeling of outer hair cell stereocilia is more prominent in other sections). Large arrowhead, inner hair cell stereocilia; small arrowheads, outer hair cell stereocilia; +, inner hair cell nuclei; *, outer hair cell nuclei; TM, tectorial membrane. All slices are 3 $\mu$m thick, imbedded in plastic, and shown at 100× magnification with Nomarski optics. Scale bar = 10 $\mu$m.

in 58% of *dfw*$^{2J}$ ($n$ = 24) and 61% of control ($n$ = 28) mice (Fig. 5B). Among the mice in which endolymph $Ca^{2+}$ concentrations were measured, the mean CB EP was 89.3 ± 7.9 mV, and the mean *dfw*$^{2J}$ EP was 61.9 ± 7.8 mV ($n$ = 8 in each group). The difference between *dfw*$^{2J}$ and CB EPs was statistically significant with a $p$ value of 0.031 determined by the two-tailed Student's $t$ test.

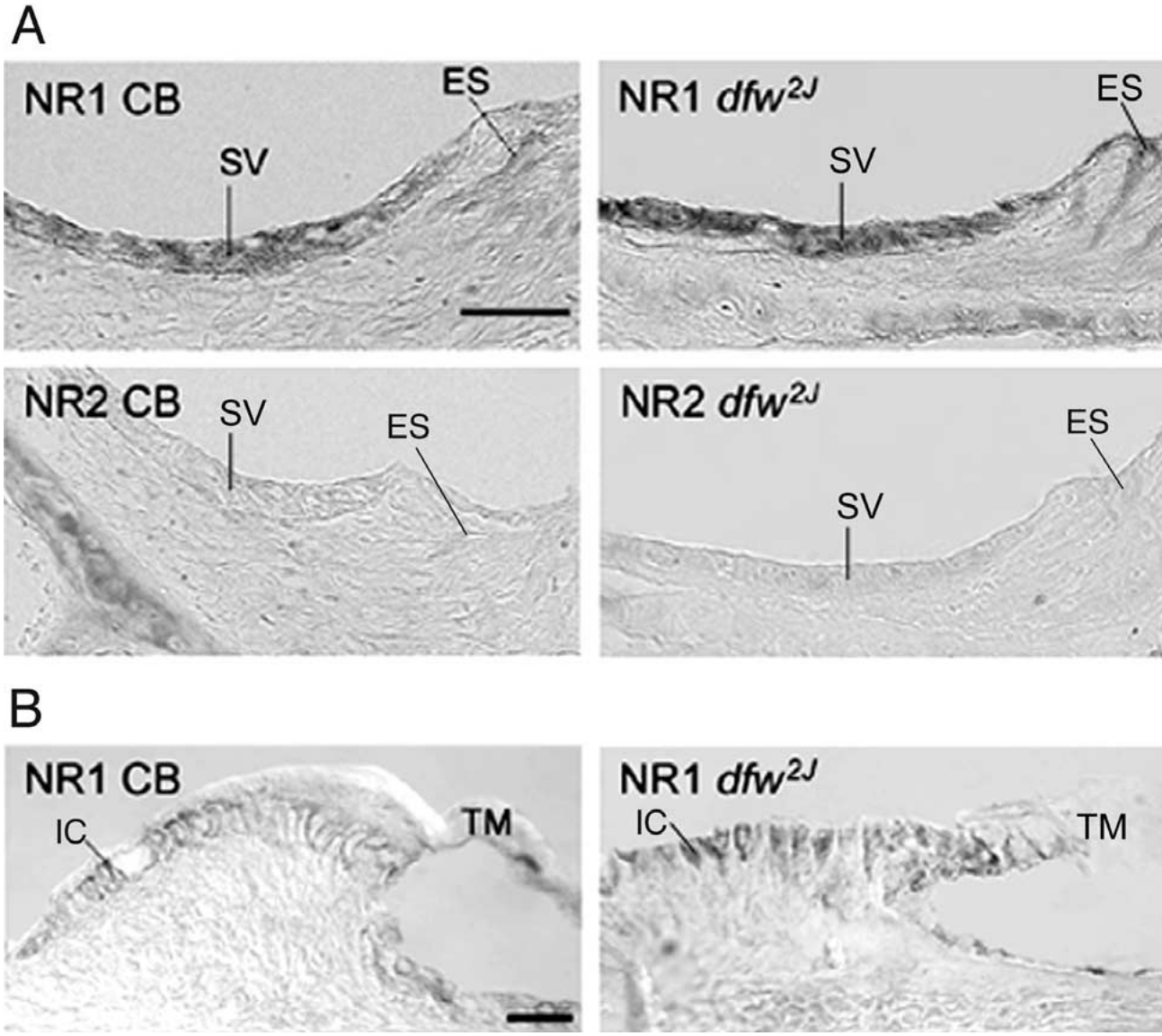


**FIG. 3.** **A** PMCA1 and PMCA2 staining in the stria vascularis. **NR1 CB** NR1 ICC for PMCA1 in CB cochlea. There is intense NR1 labeling of the stria vascularis and low-intensity labeling of the external sulcus. **NR1 dfw**$^{2J}$ NR1 ICC for PMCA1 in *dfw*$^{2J}$ cochlea. There is intense NR1 labeling of the stria vascularis and low-intensity labeling of the external sulcus. **NR2 CB** NR2 ICC for PMCA2 in CB cochlea. There is no NR2 labeling of the stria. **NR2 *dfw***$^{2J}$ NR2 ICC for PMCA2 in *dfw*$^{2J}$ cochlea. There is no NR2 labeling of the stria. SV, stria vascularis; ES, external sulcus. All slices are imbedded in plastic, 3 $\mu$m thick, and shown at 100× magnification with Nomarski optics. Scale bar = 20 $\mu$m. **B** PMCA1 ICC of spiral limbus. **NR1 CB** NR1 ICC for PMCA1 in CB cochlea. There is intense NR1 labeling of spiral limbus interdental cells. **NR1** *dfw*$^{2J}$ NR1 ICC for PMCA1 in *dfw*$^{2J}$ cochlea. There is intense NR1 labeling of interdental cells. TM, tectorial membrane; IC, interdental cells. Slices are imbedded in plastic, 3 $\mu$m thick, and shown at 63× magnification with Nomarski optics. Scale bar = 20 $\mu$m.

## DISCUSSION

Our measurements of low endolymph $Ca^{2+}$ concentrations in *dfw*$^{2J}$ mutant mice lacking functional PMCA2 suggest that PMCA2 is necessary for maintenance of normal endolymph $Ca^{2+}$ concentrations. Within the endolumenal cell layer where calcium transport into the endolymph must occur, our ICC results indicate that PMCA2 is present only in inner and outer hair cell stereocilia and outer hair cell apical membranes, indicating that these areas may be important sites of endolymph $Ca^{2+}$ regulation.

### *dfw*$^{2J}$ anatomy

The anatomic abnormalities observed in *dfw*$^{2J}$ mice are consistent with those previously reported in *dfw*$^{2J}$ (Street et al. 1998) and in mice homozygous for a targeted mutation of PMCA2 (Kozel et al. 1998). Anatomic distortion and absence of identifiable hair

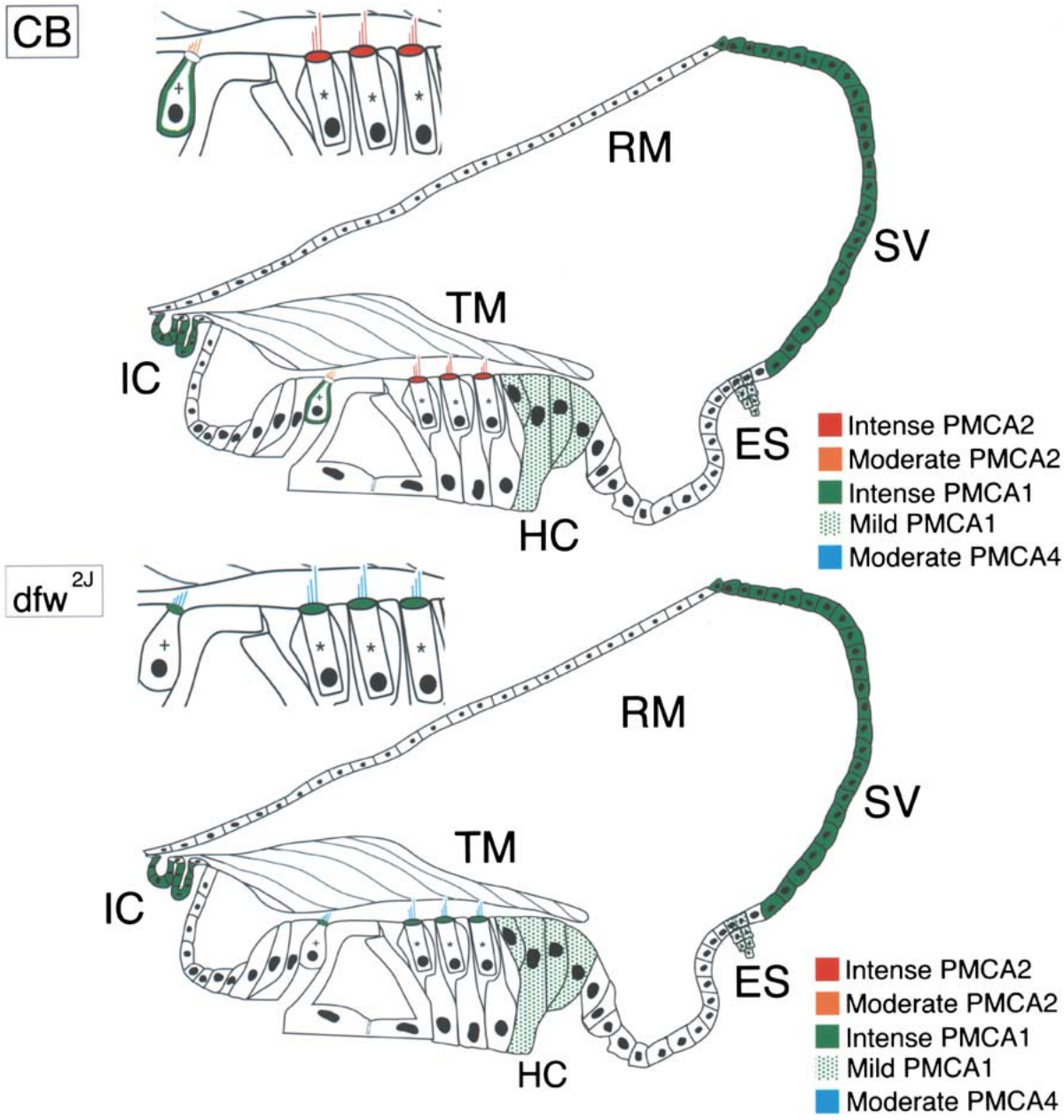


**FIG. 4.** Summary of PMCA staining. The schematics depict PMCA ICC results in the endolumenal cell layer of CB and *dfw*$^{2J}$ mice. In CB mice, intense PMCA1 labeling was present in the stria vascularis, basolateral membranes of inner hair cells, and interdental cells. Low-intensity PMCA1 labeling was present occasionally in Hensen and external sulcus cells. Intense PMCA2 labeling was present in the outer hair cell stereocilia and apical surfaces. Moderate PMCA2 labeling was present in inner hair cell stereocilia. There was no staining for PMCA4 in CB mice. In *dfw*$^{2J}$ mice, intense PMCA1 labeling was present in the stria vascularis, apical surface of inner and outer hair cells, and interdental cells. Moderate PMCA1 labeling was present occasionally in Hensen and external sulcus cells. No PMCA2 labeling was present in the *dfw*$^{2J}$ endolumenal cell layer. Moderate PMCA4 staining was present in inner and outer hair cell stereocilia. +, inner hair cells; *, outer hair cells; EC, external sulcus cells; HC, Hensen cells; IC, interdental cells; RM, Reissner's membrane; SV, stria vascularis; TM, tectorial membrane.

cells in the most affected areas of *dfw*$^{2J}$ cochleae likely contribute to the mutants' deafness, but if the observed abnormal anatomy were the only defect, portions of the cochlea with apparently normal architecture should provide some hearing. Instead, *dfw*$^{2J}$ mice are profoundly deaf at all tested frequencies (Noben–Trauth et al. 1997), suggesting additional pathology. Sporadic disruption of *dfw*$^{2J}$'s Reissner's membrane likely represents a tissue preparation artifact rather than rupture of the cochlear duct *in vivo* given that stable EPs were recorded with near equal frequency in *dfw*$^{2J}$ and in control mice and that membrane disruption was also observed in control mice.

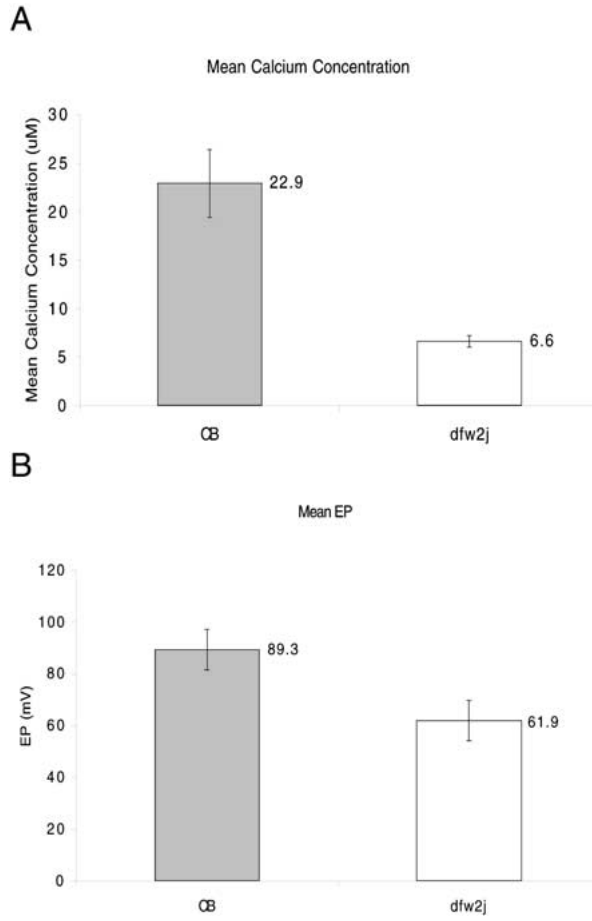


**FIG. 5.** **A** Mean endolymph calcium concentrations. The graph depicts mean calcium concentrations of endolymph samples; $n = 8$ in each group. Standard error bars are shown. **B** Mean endocochlear potentials. The graph depicts mean endocochlear potentials; $n = 8$ in each group. Standard error bars are shown.

## Immunocytochemistry

Previous immunocytochemistry experiments agree that PMCA1 is present in the stria vascularis but differ regarding localization of PMCA1 within marginal cells, the innermost stria cells that line the cochlear duct. PMCA non-type-specific labeling of marginal cells in the developing gerbil was reported as basolateral (Crouch and Schulte 1995) but, in the adult rat, labeling was demonstrated along the entire marginal cell plasma membrane (Agrup et al. 1999). Our results concur with the previous rat study, suggesting that PMCA1 is present on both apical and basolateral surfaces of marginal cells.

To our knowledge, there is no previous report of PMCA1 in spiral limbus interdental cells, which are thought to contribute to maintenance of the tectorial membrane (TM) (Spicer et al. 2000). Chelation of $Ca^{2+}$ with EDTA causes swelling of the TM (Kronester–Frei 1979) and loss of its normally organized, striated structure (Hasko and Richardson 1988). Interdental cell PMCA1 might provide localized calcium to help establish or maintain the overlying TM.

Our ICC results indicate that PMCA2 is the primary PMCA type present in wild-type mice inner and outer hair cell stereocilia, consistent with findings in the rat, which further specify that the isoform is PMCA2a (Dumont et al. 2001). Occasional PMCA1 immunolabeling of outer hair cell apical surfaces has been reported in the rat (Dumont et al. 2001), but we observed no such labeling in the wild-type mouse. Mutant *dfw*$^{2J}$ mice, however, demonstrated prominent, apical, outer hair cell, PMCA1 labeling. In addition, *dfw*$^{2J}$ mice exhibited inner hair cell, apical, PMCA1 labeling that differed markedly from the basolateral labeling that we observed in wild-type mice and that others have reported in rats (Dumont et al. 2001). The abnormal localization of PMCA1 to the apical surfaces of inner and outer hair cells of *dfw*$^{2J}$ may be a compensatory response to the loss of functional PMCA2.

PMCA3 labeling was not observed in *dfw*$^{2J}$ or CB mice but has been reported in a ring surrounding rat inner hair cell cuticular plates and occasionally in basolateral membranes and stereocilia (Dumont et al. 2001). Negative PMCA3 ICC has been reported in gerbil cochleae (Crouch and Schulte 1995), and the differences in our observations from those made in the rat may reflect interspecies variability. In the case of pericuticular labeling, confocal microscopy's ability to focus precisely on immunofluorescent labeling in the cuticular plane may have afforded Dumont et al. greater sensitivity than that provided by our light microscopy technique.

PMCA4 labeling was present in *dfw*$^{2J}$ IHC and OHC stereocilia but not in wild-type cochleae. Previous studies in the adult rat organ of Corti also report no PMCA4 ICC labeling (Dumont et al. 2001), but PMCA4 immunolabeling of inner and outer hair cells has been observed in immature PN 6, 10, and 15 CB mice organs of Corti (Muchinsky, unpublished data). *In situ* hybridization has also suggested transient PMCA4 expression in inner hair cells at PN12 (Furuta et al. 1998). These observations suggest that PMCA4 may have a developmental function and may persist in *dfw*$^{2J}$ mice in the absence of functional PMCA2.

Our immunocytochemical studies show that two different PMCA types, PMCA1 and PMCA4, both respond to the lack of PMCA2 in stereocilia of *dfw*$^{2J}$ mutants. In the case of PMCA1, expression is turned on in outer hair cells and membrane localization becomes apical in both inner and outer hair cells. For PMCA4, expression is maintained beyond its normal time of down-regulation during development. These changes may reflect shared but hierarchical sensitivity of response elements in the respective promoters, for instance to changes in cellular $Ca^{2+}$ levels or flux in

*dfw*$^{2J}$ mutant hair cells (West et al. 2002). Compensatory upregulation of related genes in a developmental pathway has been observed, classically in the Myf-5 to MyoD transition in muscle cell development (Weintraub 1993). While the mechanism(s) of the compensation seen in *dfw*$^{2J}$ remain unknown, that they occur and yet are insufficient to compensate for the loss of PMCA2 suggests that the rapid and potent pumping activity of PMCA2 is critical for its function in stereocilia (Caride et al. 2001).

### PMCA2 and endolymph $Ca^{2+}$

In adult wild-type mice, PMCA1 in the stria vascularis and interdental cells and PMCA2 in hair cells were the only PMCA types identified in the apical membranes of endolumenal cells where it is possible to transport $Ca^{2+}$ across the tight junction barrier into the endolymph. Despite high levels of PMCA1 in the stria vascularis and interdental cells, abnormal localization of PMCA1 to hair cell apical surfaces, and the presence of PMCA4 in stereocilia, *dfw*$^{2J}$ endolymph $Ca^{2+}$ concentrations are significantly lower than those of wild-type mice, suggesting that PMCA2 is necessary to maintain normal endolymph $Ca^{2+}$ levels. Thus, our findings indicate that, unlike potassium whose endolymph concentration is believed to be established by the stria vascularis (Konishi et al. 1978; Wangemann et al. 1995), $Ca^{2+}$ endolymph concentrations are maintained, at least in part, by inner and outer hair cells.

Lowered EPs may contribute to *dfw*$^{2J}$'s hearing deficit but likely do not account fully for the mutant's profound deafness. Compound action potentials (CAPs) reflect auditory nerve response to acoustic stimuli (Moller 1983). Gerbils whose EPs have been reduced to as low as 43 mV by chronic furosemide administration exhibit CAP thresholds as high as 80 dB SPL to 20,000 Hz stimuli and as low as 35 dB SPL to 3000 Hz stimuli (Schmiedt et al. 2002). *dfw*$^{2J}$'s mean EP of 61.9 mV is not as reduced as the furosemide-treated gerbil. Thus, unless mouse CAPs are more sensitive to decreases in the endocochlear potential, *dfw*$^{2J}$'s lowered EP does not account for the mutant's profound deafness with no ABR responses to stimuli up to 100 dB SPL at 8000, 16,000, and 32,000 Hz (Noben–Trauth et al. 1997). Lower EPs in *dfw*$^{2J}$ reinforce the significance of low calcium concentrations, for an isolated decrease in the EP should increase the endolymph calcium concentration.

Although our experiments do not directly determine the cause of *dfw*$^{2J}$'s deafness, they do suggest that low endolymph $Ca^{2+}$ concentrations might contribute significantly. As discussed previously, *in vitro* experiments have demonstrated that chick vestibular hair cell transduction (Ohmori 1985) and bullfrog macular epithelium microphonic currents require extracellular $Ca^{2+}$ concentrations greater than 10 $\mu$M (Corey and Hudspeth 1979). If mouse auditory hair cell extracellular $Ca^{2+}$ requirements are similar, *dfw*$^{2J}$'s 6.6 $\mu$M endolymph $Ca^{2+}$ concentration is not adequate to support transduction, unless localized concentrations of calcium surrounding the hair cells are higher than the gross endolymph concentration that we measured. Additionally, low endolymph $Ca^{2+}$ concentrations might interfere with the $Ca^{2+}$-dependent hair cell processes of adaptation and hair bundle movement. Independent of the precise etiology of *dfw*$^{2J}$'s deafness, our identification of PMCA2 in wild-type mice inner and outer hair cell stereocilia and outer hair cell apical membranes and the observation of low endolymph $Ca^{2+}$ concentrations in *dfw*$^{2J}$ mice suggest that PMCA2 in inner and outer hair cells regulates endolymph $Ca^{2+}$ concentrations.

## ACKNOWLEDGMENTS

We thank Linda Robinson, Yong Lu, David Mills, and Rosalia Fonseca Burke for advice and expert technical assistance. We also thank Josh Gittelman and Helen Brew for comments on the manuscript. This work was supported by NIH grants F32-DC00018 and P30-DC04661 and by RO1s DC02739, DC04200, and GM28835.

## REFERENCES

AGRUP C, BAGGER–SJOBACK D, FRYCKSTEDT J. Presence of plasma membrane-bound Ca(2+)–ATPase in the secretory epithelia of the inner ear. Acta Otolaryngol. 119:437–445, 1999.

ASSAD JA, HACOHEN N, COREY DP. Voltage dependence of adaptation and active bundle movement in bullfrog saccular hair cells. Proc. Natl. Acad. Sci. USA 86:2918–2922, 1989.

BERGSTROM L, JENKINS P, SANDO I, ENGLISH GM. Hearing loss in renal disease: clinical and pathological studies. Ann. Otol. Rhinol. Laryngol. 82:555–576, 1973.

BOSHER SK, WARREN RL. Very low calcium content of cochlear endolymph, an extracellular fluid. Nature 273:377–378, 1978.

BROOKES GB. Vitamin D deficiency and deafness: 1984 update. Am. J. Otol. 6:102–l07, 1985.

CARAFOLI E. Intracellular calcium homeostasis. Annu. Rev. Biochem. 56:395–433, 1987.

CARIDE AJ, FILOTEO AG, ENYEDI A, VERMA AK, PENNISTON JT. Detection of isoform 4 of the plasma membrane calcium pump in human tissues by using isoform-specific monoclonal antibodies. Biochem. J. 316:353–359, 1996.

CARIDE AJ, FILOTEO AG, PENHEITER AR, PASZTY K, ENYEDI A, PENNISTON JT. Delayed activation of the plasma membrane calcium pump by a sudden increase in Ca2+: fast pumps reside in fast cells. Cell Calcium 30:49–57, 2001.

COREY DP, HUDSPETH AJ. Ionic basis of the receptor potential in a vertebrate hair cell. Nature 281:675–677, 1979.

CROUCH JJ, SCHULTE BA. Expression of plasma membrane Ca–ATPase in the adult and developing gerbil cochlea. Hear. Res. 92:112–119, 1995.

CROUCH JJ, SCHULTE BA. Identification and cloning of site C splice variants of plasma membrane Ca–ATPase in the gerbil cochlea. Hear. Res. 101:55–61, 1996.

DUMONT RA, LINS U, FILOTEO AG, PENNISTON JT, KACHAR B, GILLESPIE PG. Plasma membrane Ca2+–ATPase isoform 2a is the PMCA of hair bundles. J. Neurosci. 21:5066–5078, 2001.

FERRARY E, TRAN BA HUY P, ROINEL N, BERNARD C, AMIEL C. Calcium and the inner ear fluids. Acta Otolaryngol. Suppl. 460:13–17, 1988.

FILOTEO AG, ELWESS NL, ENYEDI A, CARIDE A, AUNG HH, PENNISTON JT. Plasma membrane Ca2+ pump in rat brain. Patterns of alternative splices seen by isoform-specific antibodies. J. Biol. Chem. 272:23741–23747, 1997.

FURUTA H, LUO L, HEPLER K, RYAN AF. Evidence for differential regulation of calcium by outer versus inner hair cells: plasma membrane Ca–ATPase gene expression. Hear. Res. 123:10–26, 1998.

HASKO JA, RICHARDSON GP. The ultrastructural organization and properties of the mouse tectorial membrane matrix. Hear. Res. 35:21–38, 1988.

HUDSPETH AJ. How hearing happens. Neuron 19:947–950, 1997.

HUDSPETH AJ, LEWIS RS. A model for electrical resonance and frequency tuning in saccular hair cells of the bull-frog, *Rana catesbeiana*. J. Physiol. 400:275297, 1988.

IKEDA K, KUSAKARI J, TAKASAKA T. Ionic changes in cochlear endolymph of the guinea pig induced by acoustic injury. Hear. Res. 32:103–110, 1988.

IKEDA K, KUSAKARI J, KOBAYASHI T, SAITO Y. The effect of vitamin D deficiency on the cochlear potentials and the perilymphatic ionized calcium concentration of rats. Acta Otolaryngol. Suppl. 435:64–72, 1987a.

IKEDA K, KOBAYASHI T, KUSAKARI J, TAKASAKA T, YUMITA S, FURUKAWA Y. Sensorineural hearing loss associated with hypoparathyroidism. Laryngoscope 97:1075–1079, 1987b.

IKEDA K, KOBAYASHI T, ITOH Z, KUSAKARI J, TAKASAKA T. Evaluation of vitamin D metabolism in patients with bilateral sensorineural hearing loss. Am. J. Otol. 10:11–13, 1989.

JAHNKE K. The fine structure of freeze-fractured intercellular junctions in the guinea pig inner ear. Acta Otolaryngol. Suppl. 336:1–40, 1975.

JOHNSON DW, MATHOG RH. Hearing function and chronic renal failure. Ann. Otol. Rhinol. Laryngol. 85:43–49, 1976.

KEETON TP, BURK SE, SHULL GE. Alternative splicing of exons encoding the calmodulin-binding domains and C termini of plasma membrane Ca(2+)–ATPase isoforms 1, 2, 3, and 4. J. Biol. Chem. 268:2740–2748, 1993.

KONISHI T, HAMRICK PE, WALSH PJ. Ion transport in guinea pig cochlea. I. Potassium and sodium transport. Acta Otolaryngol. 86:22–34, 1978.

KOZEL PJ, FRIEDMAN RA, ERWAY LC, YAMOAH EN, LIU LH, RIDDLE T, DUFFY JJ, DOETSCHMAN T, MILLER ML, CARDELL EL, SHULL GE. Balance and hearing deficits in mice with a null mutation in the gene encoding plasma membrane Ca2+–ATPase isoform 2. J. Biol. Chem. 273:18693–18696, 1998.

KRONESTER–FREI A. The effect of changes in endolymphatic ion concentrations on the tectorial membrane. Hear. Res. 1:81–94, 1979.

LUMPKIN EA, MARQUIS RE, HUDSPETH AJ. The selectivity of the hair cell's mechanoelectrical-transduction channel promotes Ca2+ flux at low Ca2+ concentrations. Proc. Natl. Acad. Sci. USA 94:10997–11002, 1997.

MARCUS DC, GE XX, THALMAN R. Comparison of the non-adrenergic action of phentolamine with that of vanadate on cochlear function. Hear. Res. 7:233–246, 1982.

MILLER RJ. The control of neuronal Ca2+ homeostasis. Prog. Neurobiol. 37:255–285, 1991.

MOLLER AR. Auditory Physiology Academic Press New York, 1983.

NOBEN–TRAUTH K, ZHENG QY, JOHNSON KR, NISHINA PM. mdfw: a deafness susceptibility locus that interacts with deaf waddler (dfw). Genomics 44:266–272, 1997.

OHMORI H. Mechano-electrical transduction currents in isolated vestibular hair cells of the chick. J. Physiol. 359:189–217, 1985.

RICCI AJ, FETTIPLACE R. Calcium permeation of the turtle hair cell mechanotransducer channel and its relation to the composition of endolymph. J. Physiol. 506(Pt 1):159–173, 1998.

RICCI AJ, CRAWFORD AC, FETTIPLACE R. Active hair bundle motion linked to fast transducer adaptation in auditory hair cells. J. Neurosci. 20:7131–714, 2000.

SALT AN. Neurobiology of hearing: the cochlea, 1st ed. Raven Press, New York, 1986.

SCHMIEDT RA, LANG H, OKAMURA HO, SCHULTE BA. Effects of furosemide applied chronically to the round window: a model of metabolic presbyacusis. J. Neurosci. 22:9643–9650, 2002.

SPICER SS, THOMOPOULOS GN, SCHULTE BA. Structural evidence for ion transport and tectorial membrane maintenance in the gerbil limbus. Hear. Res. 143:147–161, 2000.

STREET VA, MCKEE–JOHNSON JW, FONSECA RC, TEMPEL BL, NOBEN–TRAUTH K. Mutations in a plasma membrane Ca2+–ATPase gene cause deafness in deafwaddler mice. Nat. Genet. 19:390–394, 1998.

TANAKA Y, ASANUMA A, YANAGISAWA K. Effect of EDTA in the scala media on cochlear potentials. Proc. Jpn. Acad. 55:31–36, 1979.

THORNE M, SALT AN, DEMOTT JE, HENSON MM, HENSON OW, GEWALT SL. Cochlear fluid space dimensions for six species derived from reconstructions of three-dimensional magnetic resonance images. Laryngoscope 109:1661–1668, 1999.

WANGEMANN P, LIU J, MARCUS DC. Ion transport mechanisms responsible for K+ secretion and the transepithelial voltage across marginal cells of stria vascularis *in vitro*. Hear. Res. 84:19–29, 1995.

WEINTRAUB H. The MyoD family and myogenesis: redundancy, networks, and thresholds. Cell 75:1241–1244, 1993.

WEST AE, GRIFFITH EC, GREENBERG ME. Regulation of transcription factors by neuronal activity. Nat. Rev. Neurosci. 3:921–931, 2002.

YAMOAH EN, LUMPKIN EA, DUMONT RA, SMITH PJ, HUDSPETH AJ, GILLESPIE PG. Plasma membrane Ca2+–ATPase extrudes Ca2+ from hair cell stereocilia. J. Neurosci. 18:610–624, 1998.